

ORIGINAL RESEARCH

Open Access



# Long-term biochar addition significantly decreases rice rhizosphere available phosphorus and its release risk to the environment

Hao Chen<sup>1,2†</sup>, Jiahui Yuan<sup>5†</sup>, Guanglei Chen<sup>1</sup>, Xu Zhao<sup>1,2</sup>, Shenqiang Wang<sup>1,2</sup>, Dengjun Wang<sup>3</sup>, Lei Wang<sup>4</sup>, Yujun Wang<sup>1,2</sup> and Yu Wang<sup>1,2\*</sup>

## Abstract

Phosphorus (P) availability, diffusion, and resupply processes can be altered by biochar addition in flooded rice rhizosphere, which controls the risk of P release to the environment. However, there are few in-situ investigations of these rhizospheric processes and effects. To explore the effects of biochar addition on soil P availability, high-resolution dialysis (HR-Peeper), diffusive gradients in thin films (DGT), and zymography techniques were used to provide direct evidence in the rice rhizosphere at the sub-millimeter scale. Long-term (9-years) field and greenhouse pot experiments demonstrated that biochar addition notably decreased the soluble/labile P and Fe concentrations in rice rhizosphere (vs. no biochar addition; CK) based on the results of Peeper, DGT, and two-dimensional imaging of labile P fluxes. DGT-induced fluxes in the soil/sediment (DIFS) model and sediment P release risk index (SPRRI) further indicated that biochar addition decreased the diffusion and resupply capacity of P from soil solid to the solution, thereby decreasing P release risk to the environment. These processes were dominated by Fe redox cycling and the hydrolysis of Al (hydro)oxides that greatly increased the unavailable P (Ca-P and residual-P). Additionally, greenhouse pot experiments (without additional biochar) showed that the previous long-term biochar addition significantly increased soil phosphatase activity, due to an adaptive-enhancing response to P decrease in the rhizosphere zone. The in-situ study on the biogeochemical reactions of P in the rice rhizosphere may provide a new and direct perspective to better evaluate the biochar addition and potential benefits to agricultural soils.

## Highlights

- Long-term (9-years) biochar amendment field and greenhouse pot experiments were conducted.
- DGT/DIFS/SPRRI were used to in-situ assess P availability, resupply, and release risk to the environment.
- Long-term biochar addition significantly decreased rice rhizosphere available P and its release risk to the environment.
- Fe/Al-P and unavailable P dominated the mobility and resupply of P.

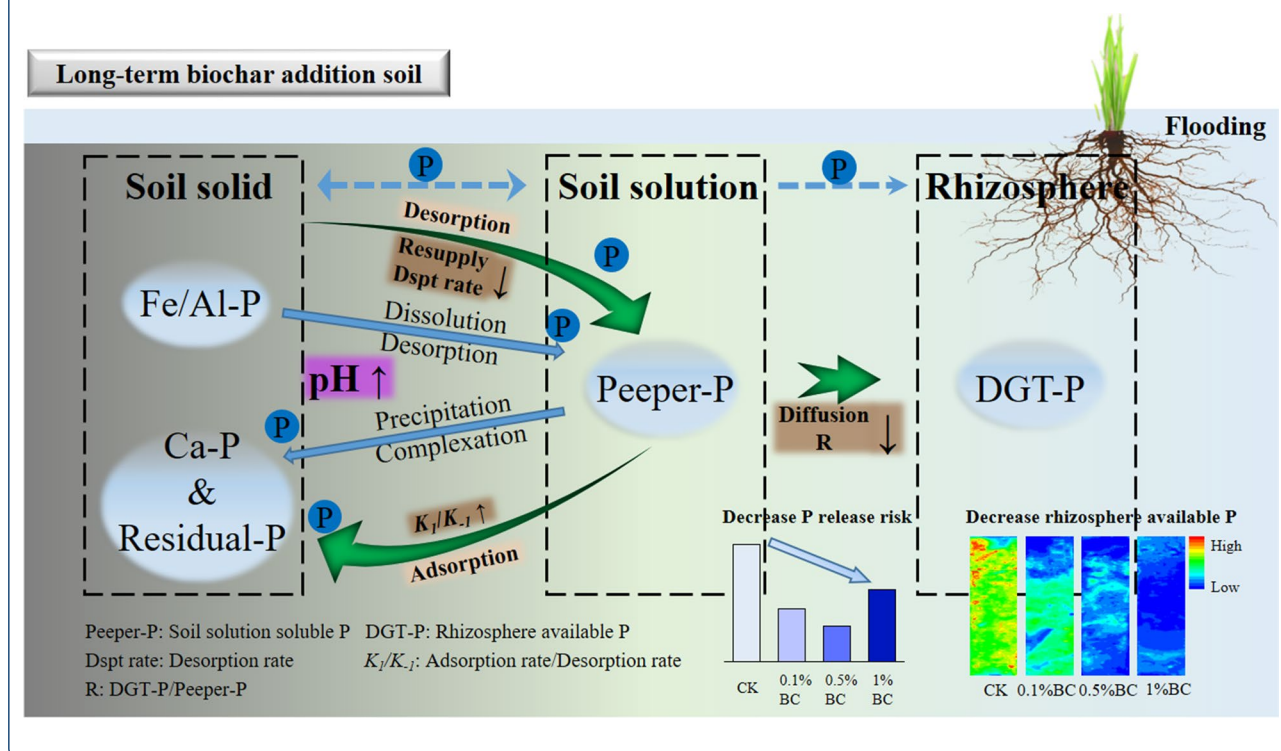
<sup>†</sup>Hao Chen and Jiahui Yuan contributed equally to this study.

\*Correspondence: wangyu@issas.ac.cn

<sup>1</sup> State Key Laboratory of Soil and Sustainable Agriculture, Changshu National Agro-Ecosystem Observation and Research Station, Institute of Soil Science, Chinese Academy of Sciences, Nanjing 210008, China  
Full list of author information is available at the end of the article

**Keywords:** Biochar, Rice rhizosphere, Phosphorus availability, DGT, DIFS, SPRII

### Graphical Abstract



## 1 Introduction

Phosphorus (P) is essential for crop growth, however, high inputs and low utilization efficiency of P fertilizers exacerbate the risk of their loss to open waters (Liu et al. 2016; Powers et al. 2016). Currently, P flow from fertilizers to erodible soils to avert the widespread eutrophication of freshwater systems has been proposed as a regional P planetary boundary (Steffen et al. 2015). Moreover, biochar is seen as an amendment in agricultural soil with growing attention, since it has great potential to increase soil carbon storage and improve soil fertility (Jeffery et al. 2011; Omondi et al. 2016), reduce greenhouse gas emission (Borchard et al. 2019), and amend the contaminated soil (Olmo et al. 2015). However, the effect of biochar addition on the release risk of P remains largely underexplored, especially in paddy fields that show a more serious P release risk to the environment compared to other arable soils (Zhang et al. 2007).

The release of P from biochar-containing soils involves complex biogeochemical processes. Almost all studies have focused on changes in soil P fractions, especially soil available P, but with different results. For instance, several recent review articles (Hossain et al. 2020; Tesfaye et al. 2021; Yang et al. 2021) summarized that biochar could increase soil available P, which might be due

to: (1) the release of P from biochar (Zhai et al. 2014), (2) promoting the desorption and dissolution of P from metal (Fe, Al) (hydro)oxides (Cui et al. 2011), and (3) stimulating the mineralization of organic P (Po) by increasing phosphatase activities (Jin et al. 2016). The observed increased amount of P was relatively lower in longer duration (>1 year) or field experiments than in short term (<1 year) or pot experiments (Gao et al. 2019). However, some studies reported that biochar addition had no significant effect (Ahmed and Schoenau 2015; Amendola et al. 2017), and even decreased the soil available P (Li et al. 2017; Xu et al. 2014). The ineffective or declined effects can be explained by the strong adsorption for P through electrostatic or binding adsorption (Xu et al. 2014), along with the formation of P precipitates by increasing soil pH (Mahmoud et al. 2020). However, the current literature on soil P cycling ignores many very important processes in the rhizosphere, which is a highly complex environment with limited information available (Jacob and Otte 2004; Yin et al. 2020). Therefore, in-situ and dynamic mapping technologies that can decipher these rhizospheric processes are vital to get direct information on the change in soil available P after biochar application in agricultural soils.

Recently, the diffusion gradients in thin films (DGT) technique has been successfully and widely applied to measure labile metals and metalloids to predict plant availability in flooded soils (Li et al. 2020; Qin et al. 2021; Santner et al. 2015; Williams et al. 2014). Additionally, Fang et al. (2021b) adopted DGT and conducted rhizobag experiments, which revealed that biochar addition reduced the bioavailability of toxic trace elements (As, Cd, and Pb) in the rice rhizosphere. However, there are relatively few in-situ studies on P in flooded paddy soils. Previous studies have only suggested that the DGT technique can be used for the in-situ distribution and variability of soil labile P around rice roots (Six et al. 2012). On this basis, we further elucidated that the availability of P in the rice rhizosphere was dominated by Fe redox cycling (Wang et al. 2019, 2021). Fang et al. (2021a) combined three high-resolution in-situ techniques and reported that P depletion around rice roots was accompanied by the stimulation of phosphatase activity and mineralization of organic P. However, direct evidence for the effect of long-term biochar addition on the distribution of available P in rice rhizosphere remains unclear.

The availability of P is influenced by both its diffusion in soil solution and its release from soil solid. These dynamic processes can be analyzed by a model of DGT-induced fluxes in sediments and soils (DIFS) (Harper et al. 1998), which has been used to accurately delineate the diffusion kinetics and resupply of metals and organic in soils and sediments (Guan et al. 2017; Li et al. 2021b; Pan et al. 2021; Xu et al. 2018). Additionally, Menezes-Blackburn et al. (2016) combined DGT and DIFS model and found that desorption rates and resupply of P from solid were significantly correlated with FeO-P, Olsen-P, and NaOH-EDTA-P. Likewise, Wu et al. (2018) observed that, in *Zizania latifolia* and *Myriophyllum verticillatum* rhizosphere, P availability was dominated by P release from Fe-P and  $\text{NH}_4\text{Cl}$ -P. Phosphorus loss from paddy soils into open waters has been regarded as an important factor for global eutrophication (Zhang et al. 2007). The conventional assessments of P mobility and potential release risk are based on the adsorption/desorption ability (Freundlich or Langmuir) (An and Li 2009) and the quantity of TP leaching, yet showing mixed results (Bradley et al. 2015; Laird et al. 2010; Li et al. 2021a). However, the reported studies neglected the underlying mechanisms of the phenomena observed after biochar addition. Wu et al. (2019) developed a sediment P release risk index (SPRRI) to evaluate the in-situ P release risk, which is based on the DIFS model and sediment chemical properties (P, Fe, and Al) and combining the labile P pool, P desorption and resupply, and Al-P. However, to date, little is known on the in-situ P release risk to the environment in long-term biochar-added paddy fields. Therefore, it is

important to understand the capacity and mechanism of the environmental impact of P release from biochar-added soils.

In this study, based on 9-years successive biochar amendment field and greenhouse pot experiments, we combined HR-Peeper, ZrO-Chelex DGT, Zr-oxide DGT, and zymography techniques to measure the P availability and identify mechanisms involved in the rice rhizosphere zone. Our objectives were to (1) investigate the direct evidence and involved mechanisms of the availability of P in rice rhizosphere induced by biochar addition on a millimeter-scale, and (2) determine the diffusion, resupply, and release risk of P from long-term biochar-added agriculture soils to the environment.

## 2 Materials and methods

### 2.1 Field experiments

#### 2.1.1 Field experimental design

The field experiments were conducted at the Yixing Base for Non-point Source Pollution Control, Changshu National Agro-Ecosystem Observation and Research Station, Chinese Academy of Sciences (119°54'E, 31°16'N), which were established in June 2010, namely, the rice-growth season. This base typically follows rice-wheat rotation and is close to Taihu Lake, with an average annual temperature and rainfall of 14.7 °C and 1174 mm, respectively. In the experiments, the biochar was prepared from rice straw by pyrolysis at 500 °C for 8 h and mixed thoroughly with the upper soil (0–20 cm) for each season. The detailed characteristics of the biochar are presented in Additional file 1: Table S1, specially, the concentration of total P and available P of biochar was 2.28 g kg<sup>-1</sup> and 221.0 mg kg<sup>-1</sup>. Four biochar treatments, including no biochar (control; CK), 2.25 t ha<sup>-1</sup> biochar (0.1%BC), 11.25 t ha<sup>-1</sup> biochar (0.5%BC), and 22.5 t ha<sup>-1</sup> biochar (1%BC) per each rice and wheat season, respectively, were arranged in a completely randomized design with three replications (n=3). Each plot was designed with an area of 4 × 5 m<sup>2</sup> separated by a 30 cm wide earth ridge. Biochar addition in each plot per season was equivalent to adding 11.8, 58.8, and 117.5 kg P<sub>2</sub>O<sub>5</sub> ha<sup>-1</sup> in 0.1%BC, 0.5%BC, and 1%BC treatments. In addition, the chemical P fertilizers were added at 60 kg P<sub>2</sub>O<sub>5</sub> ha<sup>-1</sup> and the urea fertilizers were added at 240 kg N ha<sup>-1</sup> (at tillering stage and jointing stage, basal fertilizer was applied at a ratio of 3:4:3). The basic addition rate of potassium fertilizers was 60 kg K<sub>2</sub>O ha<sup>-1</sup>.

#### 2.1.2 DGT and HR-Peeper deployment

Two types of DGT probes (an exposure window of 2 cm × 15 cm) and HR-Peeper (an exposure window of 4 cm × 20 cm) were provided by Easysensor Ltd. (Nanjing, China). The purposes of these probes are as follows:

HR-Peeper is used to simultaneously measure soluble reactive P (Peeper-P) and soluble Fe (Peeper-Fe) concentrations in soil pore water; ZrO-Chelex probe is applied to simultaneously measure soil labile P and Fe (DGT-P/Fe) concentrations (one-dimensional DGT); and Zr-oxide DGT probe is applied to measure soil labile P fluxes (two-dimensional DGT imaging) (Wang et al. 2019).

DGT probes and HR-Peeper were applied at the seedling stage (July 18, 2018, days 14 after rice transplantation) in the 2018 rice-growth season (the 9-year of the field experiments) with three replicates. Specifically, the HR-Peeper was manually inserted into the rice root zone with the least possible disturbance, and the DGT probes were inserted 24 h later. The DGT probes and HR-Peeper were taken out carefully after further stabilization for 24 h and then transported to the laboratory for further analysis. The soil temperature of each plot was 29 °C. The detailed steps of HR-Peeper and DGT sample analyses are presented in Additional file 1: Text S1.

## 2.2 Greenhouse pot experiments

### 2.2.1 Greenhouse pot experimental design

The greenhouse pot experiments were conducted in the greenhouse from July 27, 2020 to August 25, 2020, spanning 30 days of the rice seedling stage. Soil samples were collected at a depth of 0–20 cm during the wheat harvest season in 2020 and pre-aired, dried, and sieved. Each of 12 specifically designed Perspex rhizobox (10 × 8 × 20 cm<sup>3</sup> with a detachable plate) was filled with 1 kg of soil and flooded for a week before use. Two young rice seedlings of similar size were transferred into the center of each detachable plate. Then the rhizoboxes were kept inclined at an angle of 45° to make sure the root grew along with the detachable plate. Four treatments were basally fertilized with 200 mL of urea-containing solution (1 g L<sup>-1</sup>) and potassium chloride (0.877 g L<sup>-1</sup>), then top-dressed with 100 mL urea-containing solution after 2 weeks. P fertilizer was not applied this time. The soils were flooded at a depth of 3 to 5 cm during the whole experiment.

### 2.2.2 DGT and HR-Peeper deployment

The HR-Peeper was manually inserted into the rice root zone on days 1, 14, and 28 after rice transplantation for simultaneous in-situ measurement of soluble reactive P (Peeper-P) and soluble Fe (Peeper-Fe) concentrations in soil pore water. The ZrO-Chelex DGT probe was deployed adjacent to the rice roots at the same time the next day after inserting HR-Peeper to simultaneously measure soil labile P and Fe (DGT-P/Fe) concentrations (Wang et al. 2019). Both probes were taken out carefully after further stabilization for 24 h and transported to the laboratory for further

analysis. The detailed steps of HR-Peeper and DGT sample analyses are presented in Additional file 1: Text S1. After transferring the samples of two probes, the devices were returned to the rhizobox during the subsequent zymography determination to prevent changes in soil location. Subsequently, direct zymography was performed on days 3, 16, and 30 as a non-destructive technique to capture the spatial and temporal variation characteristics of enzyme activities.

### 2.2.3 Soil zymography and image processing

The in-situ measurements of soil acid and alkaline phosphatase distribution were performed according to the protocols described by Spohn and Kuzyakov (2013) and Razavi et al. (2016). The detailed steps are presented in Additional file 1: Text S2.

## 2.3 Soil P fraction and sample analyses

A sequential extraction scheme was used for P fractions according to Kopacek et al. (2005). Five P fractions include (1) H<sub>2</sub>O-P; (2) BD-P (Fe-P); (3) NaOH25-P (Al-P); (4) HCl-P (Ca-P); (5) residual-P. The detailed steps are presented in Additional file 1: Text S3.

## 2.4 DIFS model simulation

The exchange of labile P between soil solid and solution accords with the first-order kinetic equation consisting of two partial differential equations (Eqs. 1, 2) (Harper et al. 2000). Parameters of the DIFS models include diffusion layer thickness ( $\Delta g$ ), deployment time ( $T$ ), diffusion layer porosity ( $\phi_d$ ), soil porosity ( $\phi_s$ ), diffusion layer diffusion coefficient ( $D_o$ ), soil diffusion coefficient ( $D_s$ ), and soil particle concentration ( $P_c$ ).  $R$  denotes the ratio of DGT-P and Peep-P (Eq. 3) that describes the capacity of soil solid to resupply the labile P to pore water.  $K_d$  is the ratio of  $C_s$  (soil Olsen-P) and Peep-P (Eq. 4), representing the distribution coefficient of labile P between the solid phase and solution phase.  $T_c$  denotes the response time of DGT deployment (Eq. 5).

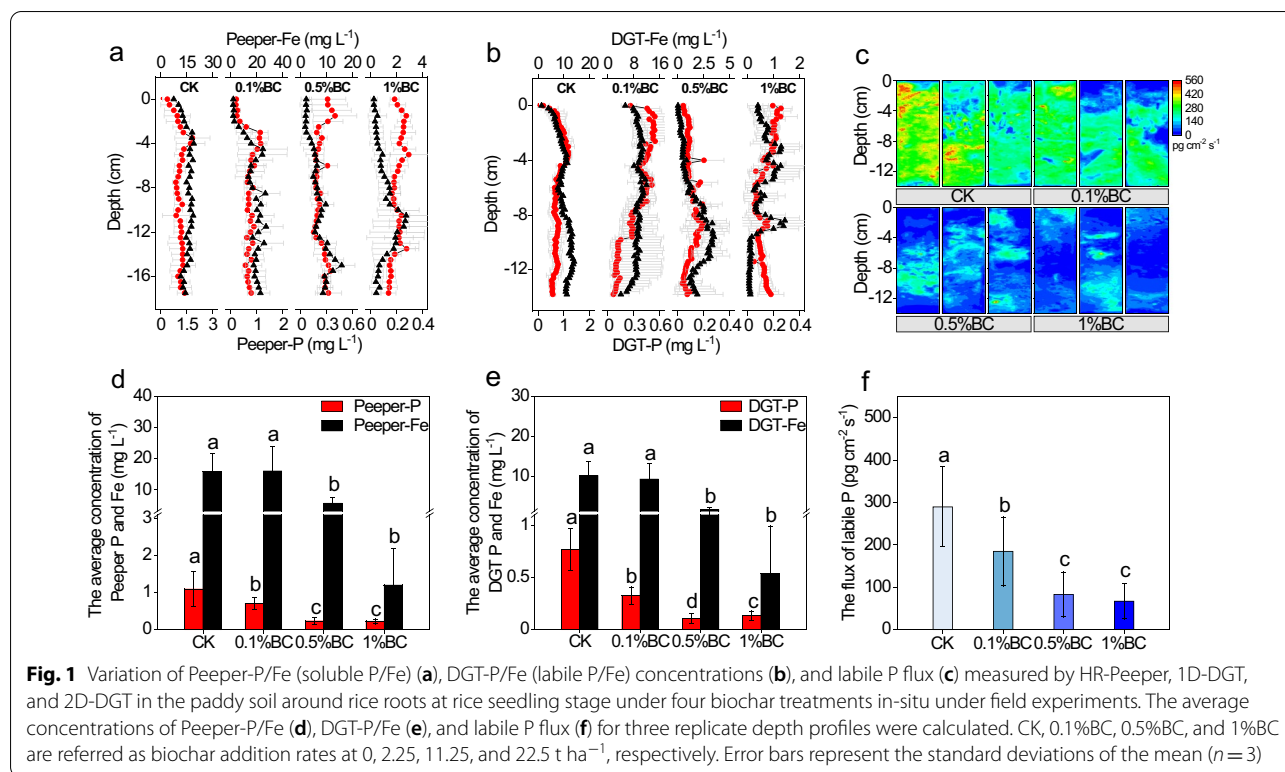
$$\frac{\partial C}{\partial t} = -kC + k_{-1}P_cC_s + D_s \frac{\partial^2 C}{\partial x^2} \quad (1)$$

$$\frac{\partial C_s}{\partial t} = \frac{k_1 C}{P_c} - k_{-1} C_s \quad (2)$$

$$R = \frac{\text{DGT} - P}{\text{Peeper} - P} \quad (3)$$

$$K_d = \frac{C_s}{\text{Peeper} - P} = \frac{1}{P_c} \times \frac{k_1}{k_{-1}} \quad (4)$$





$$T_c = \frac{1}{k_1 + k_{-1}} \tag{5}$$

$$Dspt_{rate}(\text{Desorption rate}) = \text{Olsen} - P \times P_c \times K_{-1} \tag{6}$$

where DGT-P and Peeper-P are the concentrations of soil labile P and the soil solution P determined using DGT and HR-Peeper.  $K_1$  and  $K_{-1}$  are sorption rate constant and desorption rate constant of soil particles for P, respectively. Dspt rate is the desorption rate in nmol of P per milliliter of soil solution per day.

### 2.5 SPRRI (sediment P release risk index) analysis

$$\begin{aligned} \text{SPRRI} = & 10 \times \lg(1000 \times \text{LAP/TP}) \\ & \times [R \times \lg(\text{Dspt rate})] \\ & \times \text{BD(Fe)/Al[NaOH25]} \end{aligned} \tag{7}$$

where, SPRRI [ $\lg(\text{nmol cm}^{-3} \text{d}^{-1})$ ] is an assessment index, including three parts (sub-indexes) as follows: part 1 is the  $\lg(1000 \times \text{LAP/TP})$  and represents the relative reactive P in soil phase, where LAP is the soil labile P pool (Olsen-P) and TP is soil total P; part 2 is the  $R \times \lg(\text{Dspt rate})$  and demonstrates P release from soil solid and desorption kinetics, where R is the ratio of DGT-P

and Peeper-P and Dspt rate is desorption rate; part 3 is the  $\text{BD(Fe)/Al[NaOH25]}$  (Fe/Al), which reflects the effect of Al on P release. The risk of P release index (SPRRI values) includes 5 levels: “light” (0–5), “moderate” (5–15), “relative high” (15–30), “high” (30–45), and “very high” (>45).

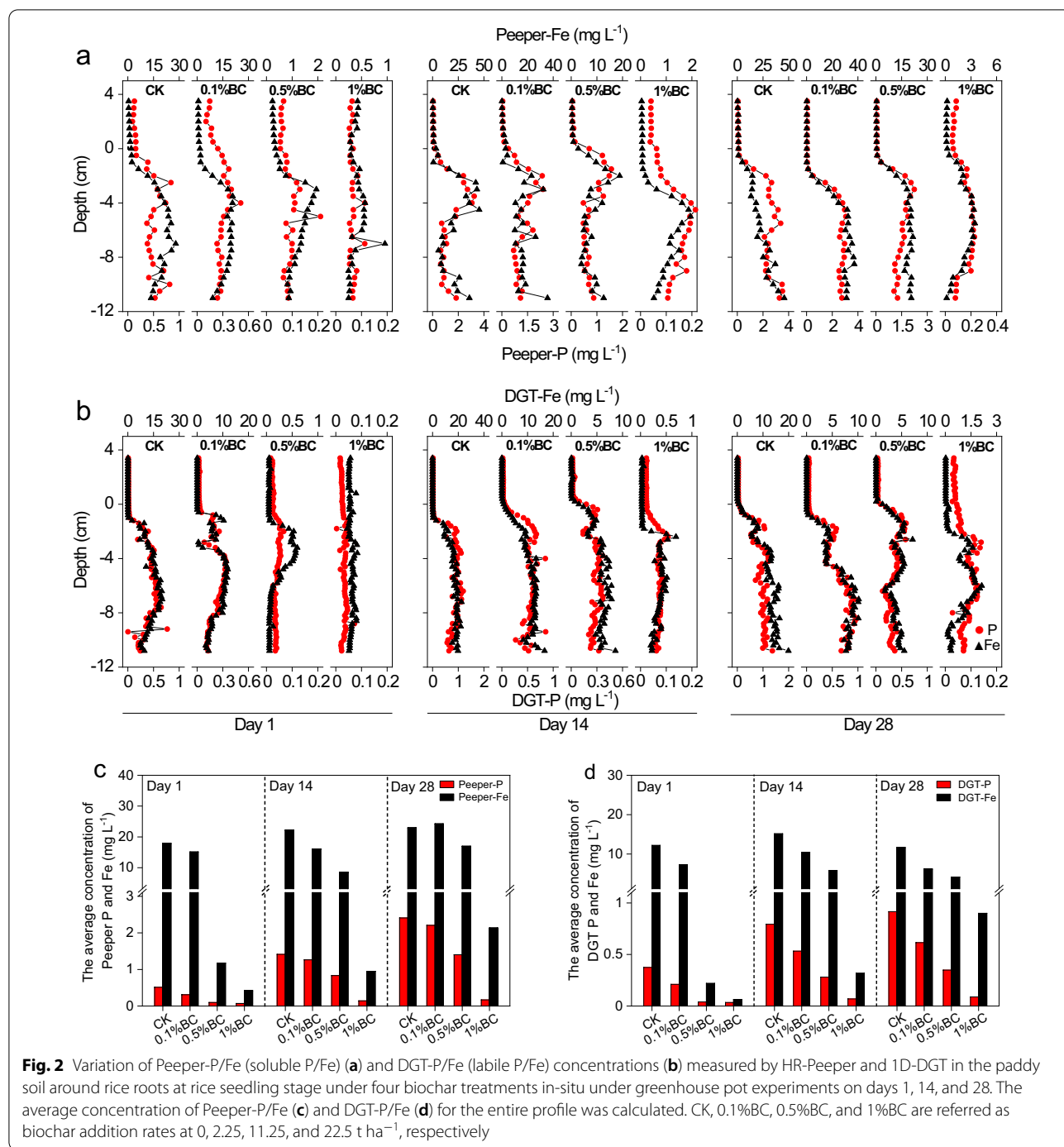
### 2.6 Statistical analysis

One-way ANOVA and the Duncan test ( $p < 0.05$  and  $p < 0.01$ ) were used to analyze the influence of biochar addition on soluble P/Fe, labile P/Fe, and P fractions among different treatments. Line regression was used to analyze the relationship between DGT P and Fe. In addition, the above statistical analyses were performed using the IBM SPSS Statistics 26.0.

## 3 Results and discussion

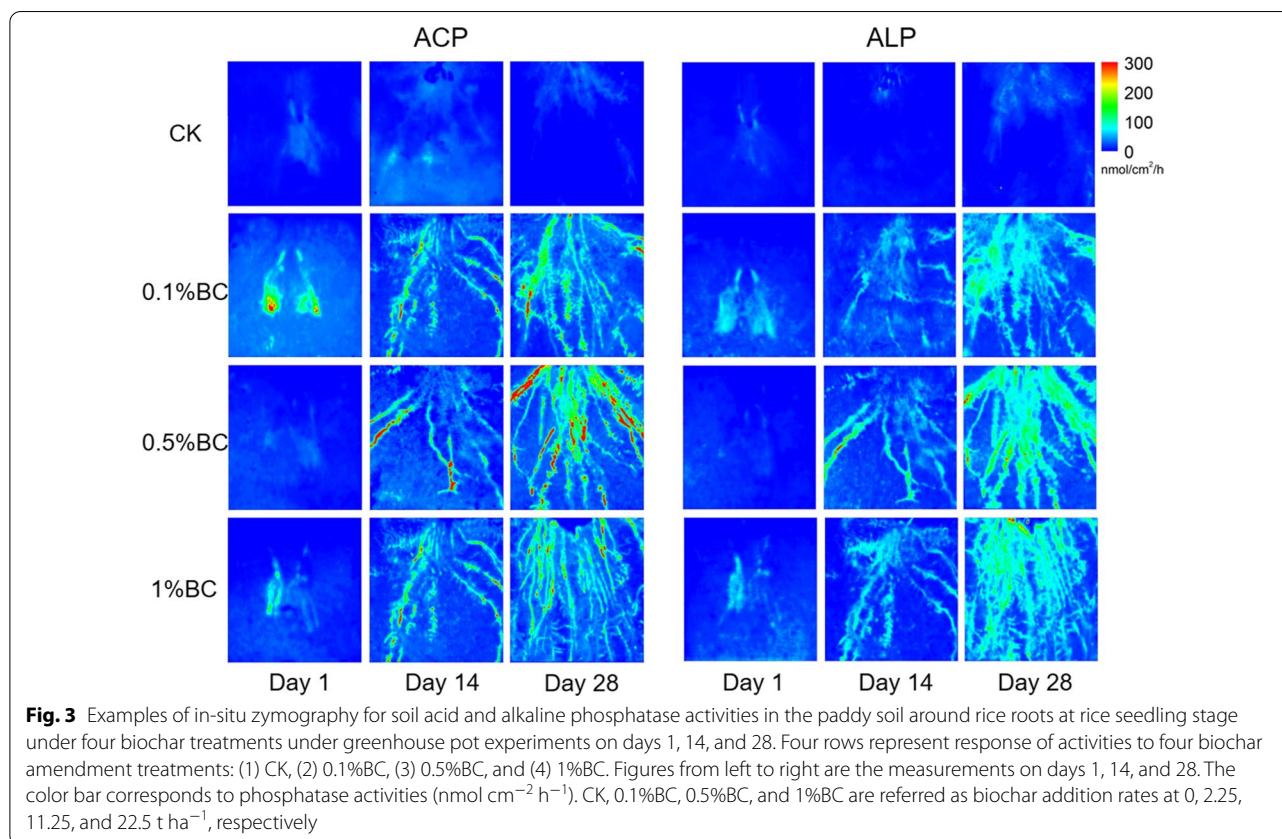
### 3.1 The variation of P availability and phosphatase activity in the rice rhizosphere

As revealed by HR-Peeper and DGT, biochar addition significantly reduced the concentrations of Peeper P and Fe in pore water, as well as DGT P and Fe in soil compared to CK (without biochar). The reduction was more significant at higher biochar addition rates, including both field and greenhouse pot experiments (Fig. 1a, b, d, and e, 2). For instance, in the field experiments, the average Peeper-P and DGT-P concentrations were reduced



by 35.4% and 57.5%, 78.9% and 86.7%, and 79.6% and 82.5% for the 0.1%BC, 0.5%BC, and 1%BC treatments, respectively, compared to CK. Furthermore, 2D visualization of labile P (represented as DGT labile P flux) (Fig. 1c) showed a highly uneven distribution of labile P in all treatments. The average flux of labile P showed similar results with Peeper-P and DGT-P (Fig. 1f),

significantly decreasing from 290 pg cm<sup>-1</sup> s<sup>-1</sup> in CK treatment to 185, 82.8, and 66.9 pg cm<sup>-1</sup> s<sup>-1</sup> in 0.1%BC, 0.5%BC, and 1%BC treatments (36.2%, 71.4%, and 76.9%, respectively). P depletion in rice rhizosphere has been confirmed in previous studies by DGT and 2D visualization imaging (Fang et al. 2021a; Wang et al. 2019; Yin et al. 2020). However, it is not clear whether biochar



addition can enhance or offset P depletion in the rice rhizosphere, especially in long-term experiments. Additionally, different experimental types and durations of biochar addition can cause huge differences in soil P availability. For example, short-term pot and incubation experiments mainly increased P availability, while there was no significant difference in field experiments (Gao et al. 2019). Hong et al. (2018) reported an increase in DGT-P content in a pot experiment with 0.6% biochar addition. In contrast, Jin et al. (2019) conducted a 5-year biochar addition field experiment—the results showed no significant change in soil P availability by biochar addition on the 5th year. In this study, the greatly decreased biochar addition on the P availability in rice rhizosphere is likely due to the decreased P diffusion and resupply from bulk soil. Moreover, biochar with a high specific surface area and alkaline cations ( $\text{Fe}^{2+}$ ,  $\text{Fe}^{3+}$ ,  $\text{Al}^{3+}$ , and  $\text{Ca}^{2+}$ ) increased the adsorption and precipitation of soil P, which further decreased the availability of P (Ghodsizad et al. 2021).

Additionally, there is a close relationship between P availability and phosphatase activities. In-situ 2D visualized zymography of phosphatase activities showed a trend opposite to P availability (Fig. 3). Soil acid

phosphatase (ACP) and alkaline phosphatase (ALP) activities in BC treatments were both up to 1.60–6.15 and 1.66–5.23 folds higher than those in CK (the increased effect of activity was greater with higher biochar addition rates). The spatial distribution of phosphatase hotspots was consistent with P decrease, suggesting that phosphatase has an adaptive increase reaction to combat P depletion in the lower P rhizosphere zone. P depletion in rice rhizosphere promoted the synthesis of phosphatase to supplement the available P with mineralized organic P. Previous studies (Fang et al. 2021a; Ma et al. 2017) used 2D in-situ zymography to visually verify the concept of a negative correlation between extracellular phosphatase activity and soil P availability (Sinsabaugh et al. 2008). Furthermore, the zones with increased ALP had further expanded away from the root surface, while ACP mainly clustered on the root surface, because soil ACP is mainly derived from plants and microorganisms, while soil ALP is mainly derived from microorganisms (Spohn and Kuzyakov 2013). The high diversity of microbes in soils could be one of the main reasons responsible for the wider distribution of ALP (Liu et al. 2017) (Table 1).

**Table 1** Characteristics of soil for four treatments under field and greenhouse pot experiments

	Pot															
	Field				Day 1				Day 14				Day 28			
	CK	0.1% BC	0.5% BC	1% BC	CK	0.1% BC	0.5% BC	1% BC	CK	0.1% BC	0.5% BC	1% BC	CK	0.1% BC	0.5% BC	1% BC
TC (g kg <sup>-1</sup> )	10.7	26.7	71.5	110	12.1	21.7	61.2	95.0	11.9	21.6	61.0	94.6	11.9	21.5	60.8	94.7
TN (g kg <sup>-1</sup> )	1.79	2.30	3.31	3.81	1.86	2.18	3.08	3.50	1.84	2.18	3.06	3.49	1.84	2.14	3.07	3.49
TP (mg kg <sup>-1</sup> )	641	569	684	814	690	561	754	803	686	574	722	780	663	583	708	791
Olsen-P (mg kg <sup>-1</sup> )	28.0	22.3	26.9	30.8	32.4	25.9	29.3	37.0	35.0	29.7	31.7	33.3	35.6	29.8	33.4	35.4
pH	6.03	6.25	6.59	6.76	5.99	6.95	7.12	7.56	6.25	6.84	7.09	7.56	6.58	7.05	7.25	7.75



**Table 2** Calculated output values for four treatments under field and greenhouse pot experiments using DIFS model

	Pot															
	Day 1			Day 14			Day 28									
	CK	0.1% BC	0.5% BC	1% BC	0.1% BC	0.5% BC	1% BC	0.1% BC	0.5% BC	1% BC	0.1% BC	0.5% BC	1% BC			
R	0.701	0.461	0.445	0.601	0.729	0.682	0.413	0.500	0.562	0.421	0.337	0.492	0.380	0.279	0.249	0.519
$K_d$ ( $\text{cm}^3 \text{g}^{-1}$ )	25.8	31.8	117	138	63.2	83.7	302	538	24.8	23.5	38.1	236	14.8	12.8	23.8	209
$T_c$ ( $10^4 \text{s}$ )	1.18	3.96	4.22	2.43	1.07	1.33	6.62	4.14	2.43	4.79	11.1	4.31	6.39	13.2	32.6	3.74
$K_1$ ( $10^{-6} \text{s}^{-1}$ )	85.8	25.3	23.8	43.7	92.3	74.6	15.1	24.1	40.3	20.4	8.8	23.1	15.1	7.30	2.98	26.7
$K_2$ ( $10^{-6} \text{s}^{-1}$ )	1.89	0.408	0.148	0.251	0.816	0.448	0.039	0.036	0.908	0.437	0.179	0.080	0.568	0.271	0.097	0.104

### 3.2 The mechanisms of the decrease in P availability and release in rice rhizosphere

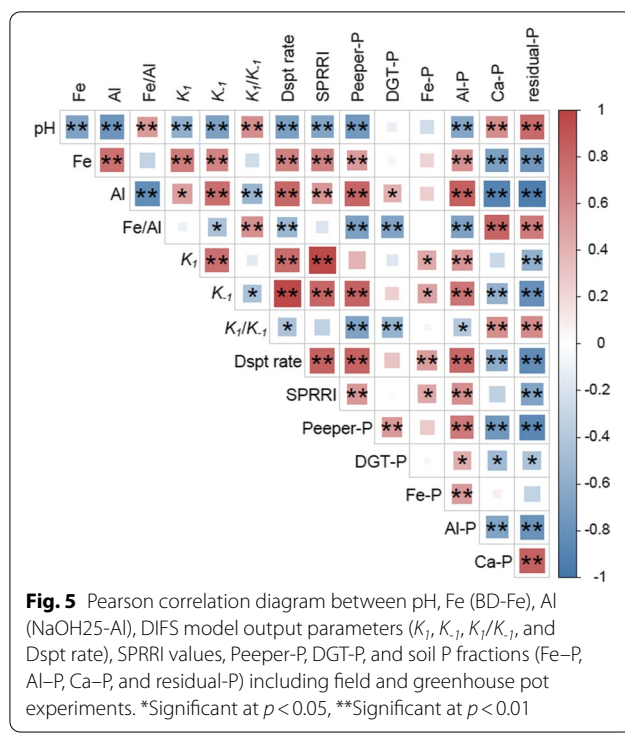
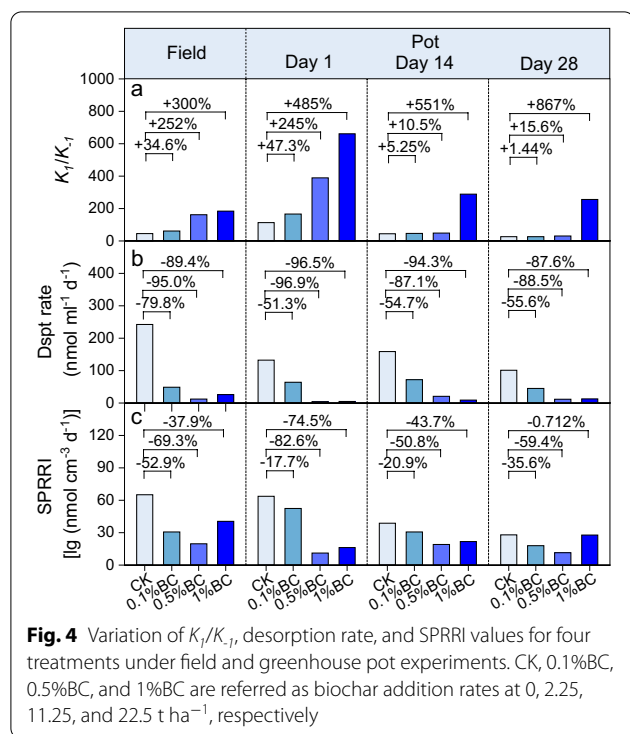
#### 3.2.1 The mobility and resupply of P evaluated according to DIFS model

In this study, the DIFS model was adopted to analyze the diffusion and resupply of P in paddy soils with long-term biochar addition (Table 2). Both the diffusion of P in the soil solution and the resupply from soil solids to the solution contributed to the R value.  $K_d$  reflects the ability of soil solid in retaining P. In the field experiments, biochar addition decreased the R values from 0.701 in CK to 0.461, 0.445, and 0.601, and increased the  $K_d$  values from 25.8 cm<sup>3</sup> g<sup>-1</sup> in CK to 31.8, 117, and 138 cm<sup>3</sup> g<sup>-1</sup>, respectively, in 0.1%BC, 0.5%BC, and 1%BC treatments. These findings suggest that biochar addition could increase the soil solid P while weakening the P resupply ability. In the DIFS model,  $T_c$  values were sensitive to the change in the R values (Lehto et al. 2008) and increased after the addition of biochar. Lower R values together with higher  $T_c$  values indicate that soil solids cannot timely and persistently provide enough P to soil solution (Yuan et al. 2021). After biochar addition, both  $K_I$  and  $K_{-I}$  values decreased significantly, but  $K_I/K_{-I}$  values increased significantly (Fig. 4a). These results showed that the sorption rather than desorption was dominated in controlling P exchange between soil solid and solution, and biochar addition reduced the desorption and resupply of labile P from soil solid to the solution (Xu et al. 2019). Therefore, the Dspt rate was significantly lower with biochar treatments compared to CK (Fig. 4b). As shown in Fig. 5, Peeper-P exhibited a significantly negative relationship with  $K_I/K_{-I}$  values ( $p < 0.01$ ), whereas a significantly positive relationship with  $K_{-I}$  values and Dspt rate ( $p < 0.01$ ), and DGT-P was also negatively correlated with  $K_I/K_{-I}$  values ( $p < 0.01$ ). The DIFS model confirmed that biochar addition reduced the P diffusion in soil solution and the P resupply from soil solid to soil solution, which further explained our previous findings on the decreased availability of P in rice rhizosphere. Similarly, a decrease in the values of R,  $K_I$ , and  $K_{-I}$  was also reported by Yang and Lu (2022) in a pot experiment with 1% biochar added at the seedling stage of rice, indicating a reduced ability of soil solids to replenish P into soil solutions. Conversely, Hong et al. (2018) conducted a pot experiment at the tillering stage of rice, and the results showed that the addition of 0.6% biochar promoted P release from soil solids to pore water due to the increased R and  $K_{-I}$  values. The reported discrepancy is likely due to the differences in the rate of biochar addition, soil physicochemical parameters such as pH, and P fractions in soil solids.

#### 3.2.2 Fe/Al/Ca bound P dominated the mobility and resupply of P

Table 3 shows the concentration and variation of bulk soil P fractions in both field and greenhouse pot experiments. As shown in the table, biochar addition significantly altered the distribution of P fractions, indicating that P has different mobility and resupply potentials in soil solids and solutions, thereby altering the availability of P in the rice rhizosphere. This was mainly due to the changes in soil pH induced by biochar addition (Fig. 5) (Biederman and Harpole 2013). The variation of soil pH significantly affected the biogeochemical processes of soil P such as adsorption–desorption, dissolution, precipitation and complexation (Eduah et al. 2019).

In this study, biochar addition decreased the concentration of Fe–P (BD-P), which indicates that biochar addition stimulated the release of Fe (hydro)oxides bound P (Kamran et al. 2019). With increasing amounts of biochar addition, the concentration of Fe (BD-Fe) decreased continuously, whereas Fe–P concentration kept increasing. This is an interesting and important observation; a possible explanation for this phenomenon may be the enhanced adsorption of Fe by biochar. Simultaneously, the increase in Fe–P might be due to the enhanced transformation of crystalline Fe oxides (goethite and hematite) to ferrihydrite (amorphous) (Eduah et al. 2019). This is because ferrihydrite (amorphous) has a much greater adsorption intensity and capacity for P than crystalline Fe oxides (goethite and hematite) and is more difficult to desorb (Ruttenberg and Sulak 2011; Zhang et al. 2003). What's more, P solubility, adsorption, and release were strongly influenced by Fe (hydro)oxides in rice ecosystems (Hossain et al. 2008). The concentrations of Fe and Fe–P showed significantly positive relationships with  $K_I$ ,  $K_{-I}$ , and Dspt rate (Fig. 5). In addition, DGT-Fe was highly positively correlated with DGT-P (Additional file 1: Fig. S2), indicating that Fe redox cycling significantly affects the release of P in paddy soils. A significant decrease of Al-P (NaOH-P) and Al (NaOH-Al) concentrations was also observed in biochar addition treatments compared to CK. This effect became more significant at higher biochar addition rates, suggesting that biochar addition promoted the hydrolysis of Al (hydro)oxides, simultaneously stimulating the release of P which bounded to Al (hydro)oxides (Kamran et al. 2019). The concentration of Al and Al-P showed significantly positive relationships with  $K_I$ ,  $K_{-I}$ , Peeper-P, DGT-P, and Dspt rate, whereas showed a significantly negative relationship with  $K_I/K_{-I}$  values (Fig. 5). These results indicated that Al-P also played an important role in P release in biochar-added paddy soils. It is worth noting that the change of Fe/Al value induced by biochar addition is one of the important factors controlling the release of P. Fe/Al value exhibited



significantly negative relationships with  $K_1$ , Dspt rate, Peeper-P, and DGT-P (Fig. 5). Furthermore, biochar addition greatly increased the concentrations of Ca-P (HCl-P) and residual-P, the proportion of which to TP increased from 20.6% in CK to 37.8%, 45.4%, and 49.5% in 0.1%BC, 0.5%BC, and 1%BC, respectively. Ca-P and residual-P are regarded as unavailable P forms in soils since they are locked in minerals and essentially “unavailable” once formed. The release of P from Fe-P and Al-P may be captured by Ca-minerals to form unavailable P due to the increase in pH induced by biochar addition (Zhai et al. 2014), thereby reducing the availability of P in the rice rhizosphere and the risk of P release to the environment (Fig. 6). Furthermore, compared to CK, the notable positive P balance in soil–plant system in biochar addition treatments was driven by P input induced by biochar addition and a slight decrease in crop uptake P (Additional file 1: Fig S3).

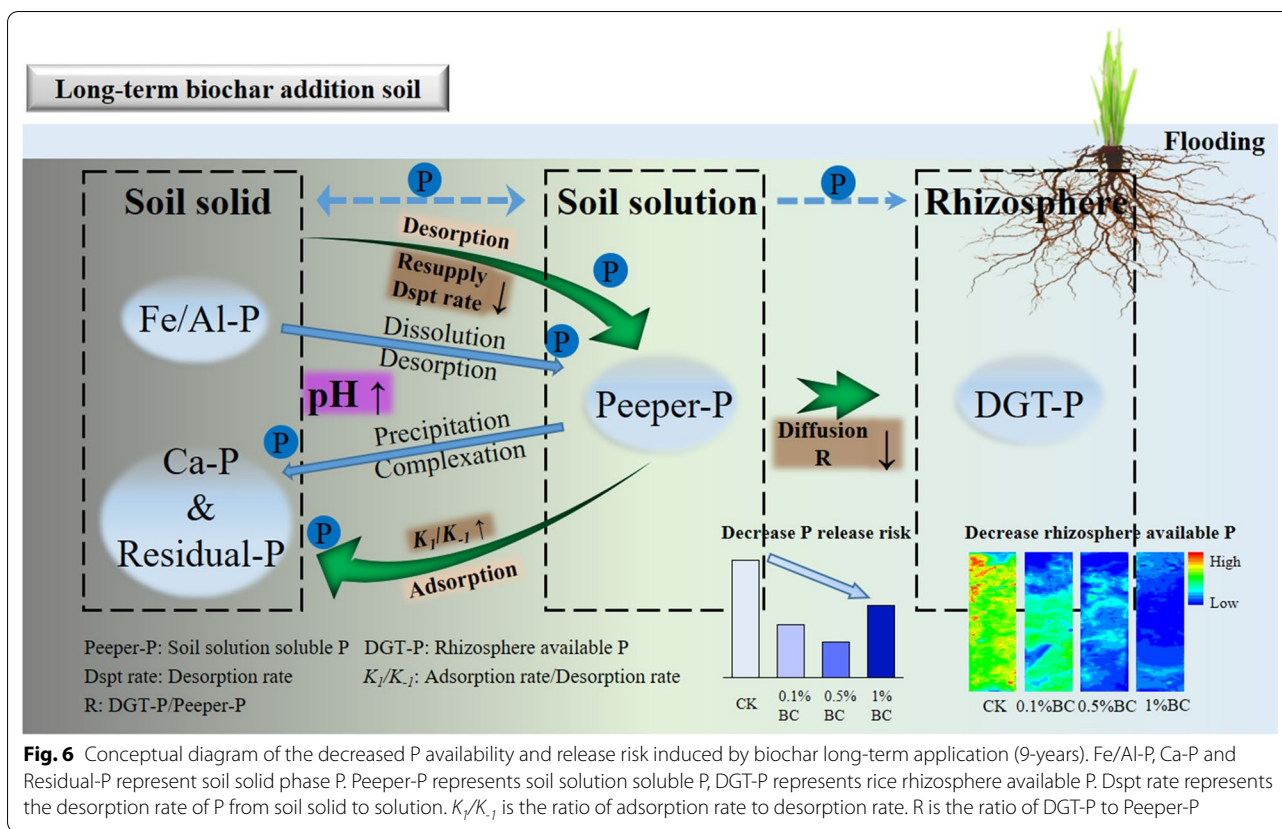
### 3.3 P release risk assessment and relevant environmental implications

Preventing the migration of P from paddy fields to freshwater systems is of great significance for controlling and reducing eutrophication. One of the most necessary strategies is to reduce the release of P from soil solids to the solution. Consequently, the in-situ research on the ability and underlying mechanisms of the solid-solution exchange of soil P is a major advance in the environmental

risk assessment of P release. In this study, SPRRI was first used to comprehensively assess the P release risk to the environment in the rice system, and it was found that biochar addition significantly decreased the soil P release risk to the environment (Fig. 4c and Additional file 1: Table S3). In field experiments, compared to CK, 0.1%BC, 0.5%BC, and 1%BC treatments decreased the SPRRI values by 52.9%, 69.3%, and 37.9%, respectively. Indeed, the CK treatment, as the conventional and prevalent application of P fertilizer, showed the highest SPRRI values, implying the most severe P release risk to the environment, at levels “very high” that even exceeded the risk of endogenous P release in lakes (Wu et al. 2019). On the contrary, the lower SPRRI values in biochar-added soils meant a relatively lower P release risk. This may be due to the transformation of soil relative available P pool to unavailable P pool and the weakening of the diffusion and resupply capacity of P from soil solid (Fig. 6). The above could be confirmed by the significantly positive relationships between SPRRI values and  $K_1$ ,  $K_1$ , Dspt rate, Peeper-P, Fe-P, and Al-P (Fig. 5). Recently, biochar or modified biochar, as a novel material for environmental remediation, has been widely used to remove P from wastewater and eutrophic lakes (Hale et al. 2013; Zhang et al. 2020). This paper highlights the roles of biochar addition in regulating P diffusion, transformation, and release in soil, so as to comprehensively assess the P release risk to the environment. With the increasing amount of biochar addition

**Table 3** The variation of soil P fraction, BD-Fe, and NaOH25-Al for four treatments under field and greenhouse pot experiments

	Field															
	Pot						Field									
	Day 1		Day 14		Day 28		Day 1		Day 14		Day 28					
CK	0.1% BC	0.5% BC	1% BC	CK	0.1% BC	0.5% BC	1% BC	CK	0.1% BC	0.5% BC	1% BC	CK	0.1% BC	0.5% BC	1% BC	
Fe-P (mg kg <sup>-1</sup> )	257	146	177	216	260	124	206	209	253	152	175	213	219	159	174	215
Al-P	250	207	194	187	254	215	203	196	274	194	208	176	245	195	205	186
Ca-P	74.5	77.9	120	177	82.7	84.2	121	154	73.5	92.2	122	152	78.8	88.5	110	149
Residual-P	57.6	137	191	227	91.4	133	220	243	83.8	133	216	237	118	133	217	238
BD-Fe	4219	3923	3639	3210	4475	3996	3664	3506	3542	3445	3341	3315	3550	3386	3284	3420
NaOH25-Al	1869	1591	1421	1063	1819	1567	1329	1193	1934	1511	1275	1174	1674	1481	1281	1161



and the requirement for more sustainable utilization of P resources, there is an increasing demand for a better understanding of P biogeochemical behavior in biochar-added soil, especially at the long-term field scale. Here, inconsistent with the most *ex-situ* studies, this paper applied DGT, DIFS model, and SPRRI as tools to investigate the fine-scale distributions and the solid-solution exchange kinetics of soil P, and further assess the P release risk to the environment. This systematic work provides a new perspective for understanding the P biogeochemical behavior in long-term biochar-added paddy soil, which helps us to better understand the P availability in rice rhizosphere, the mobility/retention of P in soils, and the environmental effects.

#### 4 Conclusions

In this study, we adopted in-situ DGT and HR-Peeper to investigate the P supply, while simultaneously observing the phosphatase activity in the rice rhizosphere under long-term biochar addition. Evidence that Peeper-P, DGT-P, and labile P flux were notably decreased and phosphatase activity was remarkably increased indicated that biochar addition significantly reduced the rice rhizosphere P availability. The DIFS model coupled with SPRRI was used to derive the P transfer and P release risk. The results

showed that biochar addition significantly decreased the diffusion and resupply of P and decreased the P release risk. Additionally, Fe redox cycling, hydrolysis of Al (hydro)oxides bound P, and the increase of unavailable P dominated the mobility and resupply of P. Research on the localized biogeochemical cycle of P and the assessment of environmental release risk in the rice rhizosphere advances our understanding on the impact of biochar addition mode on the nutrient cycle in paddy soils.

#### Supplementary Information

The online version contains supplementary material available at <https://doi.org/10.1007/s42773-022-00178-7>.

**Additional file 1.** Supplementary tables and figures.

#### Acknowledgements

Not applicable.

#### Author contributions

HC: Investigation, Formal analysis, Methodology, Writing—original draft. JY: Investigation, Formal analysis, Methodology, Writing. GC: Formal analysis, Methodology. DW: Writing—review and editing. XZ: Conceptualization, Investigation, Supervision, Writing—review and editing. SW: Conceptualization, Investigation, Supervision, Writing—review and editing. LW: Writing—review and editing. YW: Writing—review and editing. YW: Conceptualization, Investigation, Formal analysis, Funding acquisition, Supervision, Writing—review and



editing. All authors read and approved the final manuscript. All authors read and approved the final manuscript.

### Funding

This work was funded by the National Natural Science Foundation of China (No. 42277026), the National Key Research and Development Program of China (2021YFD1700802), and the Strategic Priority Research Program of the Chinese Academy of Sciences (Grant No. XDA28090300).

### Availability of data and materials

All data generated or analyzed during this study are available from the corresponding author on reasonable request.

### Declarations

#### Competing interests

The authors declare that they have no known competing financial interests or personal relationships that could have appeared to influence the work reported in this paper.

#### Author details

<sup>1</sup>State Key Laboratory of Soil and Sustainable Agriculture, Changshu National Agro-Ecosystem Observation and Research Station, Institute of Soil Science, Chinese Academy of Sciences, Nanjing 210008, China. <sup>2</sup>University of the Chinese Academy of Sciences, Beijing 10049, China. <sup>3</sup>School of Fisheries, Aquaculture and Aquatic Sciences, Auburn University, Auburn, AL 36849, USA. <sup>4</sup>Nanjing Institute of Environmental Sciences, Ministry of Ecology and Environment, Nanjing 210042, China. <sup>5</sup>Heilongjiang Academy of Black Soils Conservation and Utilization, Key Laboratory of Soil Environment and Plant Nutrition of Heilongjiang Province, Heilongjiang Academy of Agricultural Sciences, Harbin 150086, China.

Received: 19 April 2022 Accepted: 27 August 2022

Published online: 19 September 2022

### References

- Ahmed HP, Schoenau JJ (2015) Effects of biochar on yield, nutrient recovery, and soil properties in a Canola (*Brassica napus L.*)-wheat (*Triticum aestivum L.*) rotation grown under controlled environmental conditions. *Bioenergy Res* 8:1183–1196
- Amendola C, Montagnoli A, Terzaghi M, Trupiano D, Oliva F, Baronti S, Miglietta F, Chiatante D, Scippa GS (2017) Short-term effects of biochar on grapevine fine root dynamics and arbuscular mycorrhizae production. *Agr Ecosyst Environ* 239:236–245
- An WC, Li XM (2009) Phosphate adsorption characteristics at the sediment-water interface and phosphorus fractions in Nansi Lake, China, and its main inflow rivers. *Environ Monit Assess* 148:173–184
- Biederman LA, Harpole WS (2013) Biochar and its effects on plant productivity and nutrient cycling: a meta-analysis. *GCB Bioenergy* 5:202–214
- Borchard N, Schirrmann M, Cayuela ML, Kammann C, Wrage-Monnig N, Estavillo JM, Fuertes-Mendizabal T, Sigua G, Spokas K, Ippolito JA, Novak J (2019) Biochar, soil and land-use interactions that reduce nitrate leaching and N<sub>2</sub>O emissions: a meta-analysis. *Sci Total Environ* 651:2354–2364
- Bradley A, Larson RA, Runge T (2015) Effect of wood biochar in manure-applied sand columns on leachate quality. *J Environ Qual* 44:1720–1728
- Cui HJ, Wang MK, Fu M, Ci E (2011) Enhancing phosphorus availability in phosphorus-fertilized zones by reducing phosphate adsorbed on ferrihydrite using rice straw-derived biochar. *J Soil Sediment* 11:1135–1141
- Eduah JO, Nartey EK, Abekoe MK, Breuning-Madsen H, Andersen MN (2019) Phosphorus retention and availability in three contrasting soils amended with rice husk and corn cob biochar at varying pyrolysis temperatures. *Geoderma* 341:10–17
- Fang W, Williams PN, Zhang H, Yang Y, Yin DX, Liu ZD, Sun HT, Luo J (2021a) Combining multiple high-resolution in situ techniques to understand phosphorous availability around rice roots. *Environ Sci Technol* 55:13082–13092
- Fang W, Yang Y, Wang HL, Yang DX, Luo J, Williams PN (2021b) Rice rhizospheric effects on the bioavailability of toxic trace elements during land application of biochar. *Environ Sci Technol* 55:7344–7354
- Gao S, DeLuca TH, Cleveland CC (2019) Biochar additions alter phosphorus and nitrogen availability in agricultural ecosystems: a meta-analysis. *Sci Total Environ* 654:463–472
- Ghodsad L, Reyhanitabar A, Maghsoodi MR, Asgari Lajayer B, Chang SX (2021) Biochar affects the fate of phosphorus in soil and water: a critical review. *Chemosphere* 283:131176
- Guan DX, Zheng JL, Luo J, Zhang H, Davison W, Ma LQ (2017) A diffusive gradients in thin-films technique for the assessment of bisphenols desorption from soils. *J Hazard Mater* 331:321–328
- Hale SE, Alling V, Martinsen V, Mulder J, Breedveld GD, Cornelissen G (2013) The sorption and desorption of phosphate-P, ammonium-N and nitrate-N in cacao shell and corn cob biochars. *Chemosphere* 91:1612–1619
- Harper MP, Davison W, Zhang H, Tych W (1998) Kinetics of metal exchange between solids and solutions in sediments and soils interpreted from DGT measured fluxes. *Geochim Cosmochim Acta* 62:2757–2770
- Harper MP, Davison W, Tych W (2000) DIFS—a modelling and simulation tool for DGT induced trace metal remobilisation in sediments and soils. *Environ Modell Softw* 15:55–66
- Hong C, Su Y, Lu SG (2018) Phosphorus availability changes in acidic soils amended with biochar, fly ash, and lime determined by diffusive gradients in thin films (DGT) technique. *Environ Sci Pollut Res Int* 25:30547–30556
- Hossain MB, Jahiruddin M, Loeppert RH, Panaullah GM, Islam MR, Duxbury JM (2008) The effects of iron plaque and phosphorus on yield and arsenic accumulation in rice. *Plant Soil* 317:167–176
- Hossain MZ, Bahar MM, Sarkar B, Donne SW, Ok YS, Palansooriya KN, Kirkham MB, Chowdhury S, Bolan N (2020) Biochar and its importance on nutrient dynamics in soil and plant. *Biochar* 2:379–420
- Jacob DL, Otte ML (2004) Long-term effects of submergence and wetland vegetation on metals in a 90-year old abandoned Pb-Zn mine tailings pond. *Environ Pollut* 130:337–345
- Jeffery S, Verheijen FGA, van der Velde M, Bastos AC (2011) A quantitative review of the effects of biochar application to soils on crop productivity using meta-analysis. *Agr Ecosyst Environ* 144:175–187
- Jin Y, Liang XQ, He MM, Liu Y, Tian GM, Shi JY (2016) Manure biochar influence upon soil properties, phosphorus distribution and phosphatase activities: a microcosm incubation study. *Chemosphere* 142:128–135
- Jin ZW, Chen C, Chen XM, Jiang F, Hopkins I, Zhang XL, Han ZQ, Billy G, Benavides J (2019) Soil acidity, available phosphorus content, and optimal biochar and nitrogen fertilizer application rates: a five-year field trial in upland red soil, China. *Field Crop Res* 232:77–87
- Kamran MA, Xu R-K, Li J-y, Jiang J, Shi R-Y (2019) Impacts of chicken manure and peat-derived biochars and inorganic P alone or in combination on phosphorus fractionation and maize growth in an acidic ultisol. *Biochar* 1:283–291
- Kopacek J, Borovec J, Hejzlar J, Ulrich KU, Norton SA, Amirbahman A (2005) Aluminum control of phosphorus sorption by lake sediments. *Environ Sci Technol* 39:8784–8789
- Laird D, Fleming P, Wang BQ, Horton R, Karlen D (2010) Biochar impact on nutrient leaching from a Midwestern agricultural soil. *Geoderma* 158:436–442
- Lehto NJ, Sochaczewski L, Davison W, Tych W, Zhang H (2008) Quantitative assessment of soil parameter ( $K_d$  and  $T_d$ ) estimation using DGT measurements and the 2D DIFS model. *Chemosphere* 71:795–801
- Li SL, Liang CY, Shangguan ZP (2017) Effects of apple branch biochar on soil C mineralization and nutrient cycling under two levels of N. *Sci Total Environ* 607–608:109–119
- Li K, Liu Z, Shi X, Wei TJ, Ma LQ, Luo J (2020) Novel in situ method based on diffusive gradients in thin-films with lanthanum oxide nanoparticles for measuring As, Sb, and V and in waters. *J Hazard Mater* 383:121196
- Li FY, Jin YB, He S, Jin JW, Wang ZW, Khan S, Tian GM, Liang XQ (2021a) Use of polyacrylamide modified biochar coupled with organic and chemical fertilizers for reducing phosphorus loss under different cropping systems. *Agr Ecosyst Environ* 310:107306
- Li YY, Han C, Luo J, Jones KC, Zhang H (2021b) Use of the dynamic technique DGT to determine the labile pool size and kinetic resupply of pesticides in soils and sediments. *Environ Sci Technol* 55:9591–9600

- Liu X, Sheng H, Jiang SY, Yuan ZW, Zhang CS, Elser JJ (2016) Intensification of phosphorus cycling in China since the 1600s. *Proc Natl Acad Sci USA* 113:2609–2614
- Liu SB, Razavi BS, Su X, Maharjan M, Zarebanadkouki M, Blagodatskaya E, Kuzyakov Y (2017) Spatio-temporal patterns of enzyme activities after manure application reflect mechanisms of niche differentiation between plants and microorganisms. *Soil Biol Biochem* 112:100–109
- Ma XM, Razavi BS, Holz M, Blagodatskaya E, Kuzyakov Y (2017) Warming increases hotspot areas of enzyme activity and shortens the duration of hot moments in the root-detritusphere. *Soil Biol Biochem* 107:226–233
- Mahmoud E, El Baroudy A, Ali N, Sleem M (2020) Spectroscopic studies on the phosphorus adsorption in salt-affected soils with or without nano-biochar additions. *Environ Res* 184:109277
- Menezes-Blackburn D, Zhang H, Stutter M, Giles CD, Darch T, George TS, Shand C, Lumsdon D, Blackwell M, Wearing C, Cooper P, Wendler R, Brown L, Haygarth PM (2016) A holistic approach to understanding the desorption of phosphorus in soils. *Environ Sci Technol* 50:3371–3381
- Olmo M, Villar R, Salazar P, Alburquerque JA (2015) Changes in soil nutrient availability explain biochar's impact on wheat root development. *Plant Soil* 399:333–343
- Omondi MO, Xia X, Nahayo A, Liu XY, Korai PK, Pan GX (2016) Quantification of biochar effects on soil hydrological properties using meta-analysis of literature data. *Geoderma* 274:28–34
- Pan F, Cai Y, Guo Z, Fu Y, Wu X, Liu H, Wang X (2021) Kinetic characteristics of mobile Mo associated with Mn, Fe and S redox geochemistry in estuarine sediments. *J Hazard Mater* 418:126200
- Powers SM, Bruulsema TW, Burt TP, Chan NI, Elser JJ, Haygarth PM, Howden NJK, Jarvie HP, Lyu Y, Peterson HM, Sharpley Andrew N, Shen J, Worrall F, Zhang F (2016) Long-term accumulation and transport of anthropogenic phosphorus in three river basins. *Nat Geosci* 9:353–356
- Qin J, Niu A, Liu Y, Lin C (2021) Arsenic in leafy vegetable plants grown on mine water-contaminated soils: uptake, human health risk and remedial effects of biochar. *J Hazard Mater* 402:123488
- Razavi BS, Zarebanadkouki M, Blagodatskaya E, Kuzyakov Y (2016) Rhizosphere shape of lentil and maize: spatial distribution of enzyme activities. *Soil Biol Biochem* 96:229–237
- Ruttenberg KC, Sulak DJ (2011) Sorption and desorption of dissolved organic phosphorus onto iron (oxyhydr)oxides in seawater. *Geochim Cosmochim Acta* 75:4095–4112
- Santner J, Larsen M, Kreuzeder A, Glud RN (2015) Two decades of chemical imaging of solutes in sediments and soils—a review. *Anal Chim Acta* 878:9–42
- Sinsabaugh RL, Lauber CL, Weintraub MN, Ahmed B, Allison SD, Crenshaw C, Contosta AR, Cusack D, Frey S, Gallo ME, Gartner TB, Hobbie SE, Holland K, Keeler BL, Powers JS, Stursova M, Takacs-Vesbach C, Waldrop MP, Wallenstein MD, Zak DR, Zeglin LH (2008) Stoichiometry of soil enzyme activity at global scale. *Ecol Lett* 11:1252–1264
- Six L, Smolders E, Merckx R (2012) The performance of DGT versus conventional soil phosphorus tests in tropical soils—maize and rice responses to P application. *Plant Soil* 366:49–66
- Spohn M, Kuzyakov Y (2013) Distribution of microbial- and root-derived phosphatase activities in the rhizosphere depending on P availability and C allocation—coupling soil zymography with 14-C imaging. *Soil Biol Biochem* 67:106–113
- Steffen W, Richardson K, Rockstrom J, Cornell SE, Fetzer I, Bennett EM, Biggs R, Carpenter SR, de Vries W, de Wit CA, Folke C, Gerten D, Heinke J, Mace GM, Persson LM, Ramanathan V, Reyers B, Sorlin S (2015) Planetary boundaries: guiding human development on a changing planet. *Science* 347:1259855
- Tesfaye F, Liu XY, Zheng JF, Cheng K, Bian RJ, Zhang XH, Li LQ, Drosos M, Joseph S, Pan GX (2021) Could biochar amendment be a tool to improve soil availability and plant uptake of phosphorus? A meta-analysis of published experiments. *Environ Sci Pollut Res Int* 28:34108–34120
- Wang Y, Yuan JH, Chen H, Zhao X, Wang DJ, Wang SQ, Ding SM (2019) Small-scale interaction of iron and phosphorus in flooded soils with rice growth. *Sci Total Environ* 669:911–919
- Wang Y, Chen H, Wang L, Zhu WB, Yuan JH, Jaisi DP, Zhao X, Wang SQ (2021) Using diffusive gradients in thin films technique for in-situ measurement of labile phosphorus around *Oryza sativa* L. roots in flooded paddy soils. *Pedosphere* 31:76–82
- Williams PN, Santner J, Larsen M, Lehto NJ, Oburger E, Wenzel W, Glud RN, Davison W, Zhang H (2014) Localized flux maxima of arsenic, lead, and iron around root apices in flooded lowland rice. *Environ Sci Technol* 48:8498–8506
- Wu ZH, Wang SR, Luo J (2018) Transfer kinetics of phosphorus (P) in macrophyte rhizosphere and phytoremoval performance for lake sediments using DGT technique. *J Hazard Mater* 350:189–200
- Wu ZH, Wang SR, Ji NN (2019) Phosphorus (P) release risk in lake sediment evaluated by DIFS model and sediment properties: a new sediment P release risk index (SPRRI). *Environ Pollut* 255:113279
- Xu G, Sun JN, Shao HB, Chang SX (2014) Biochar had effects on phosphorus sorption and desorption in three soils with differing acidity. *Ecol Eng* 62:54–60
- Xu QY, Gao L, Peng W, Gao B, Xu DY, Sun K (2018) Assessment of labile Zn in reservoir riparian soils using DGT, DIFS, and sequential extraction. *Ecotoxicol Environ Saf* 160:184–190
- Xu DY, Gao B, Peng WQ, Gao L, Wan XH, Li YY (2019) Application of DGT/DIFS and geochemical baseline to assess Cd release risk in reservoir riparian soils, China. *Sci Total Environ* 646:1546–1553
- Yang CD, Lu SG (2022) The dynamic changes of phosphorus availability in straw/biochar-amended soils during the rice growth revealed by a combination of chemical extraction and DGT technique. *J Soil Sediment* 22:957–967
- Yang L, Wu YC, Wang YC, An WQ, Jin J, Sun K, Wang XK (2021) Effects of biochar addition on the abundance, speciation, availability, and leaching loss of soil phosphorus. *Sci Total Environ* 758:143657
- Yin DX, Fang W, Guan DX, Williams PN, Moreno-Jimenez E, Gao Y, Zhao FJ, Ma LQ, Zhang H, Luo J (2020) Localized intensification of Arsenic release within the emergent rice rhizosphere. *Environ Sci Technol* 54:3138–3147
- Yuan HZ, Wang HX, Zhou YW, Jia BC, Yu JH, Cai YW, Yang Z, Liu EF, Li Q, Yin HB (2021) Water-level fluctuations regulate the availability and diffusion kinetics process of phosphorus at lake water-sediment interface. *Water Res* 200:117258
- Zhai LM, Caiji ZM, Liu J, Wang HY, Ren TZ, Gai XP, Xi B, Liu HB (2014) Short-term effects of maize residue biochar on phosphorus availability in two soils with different phosphorus sorption capacities. *Biol Fert Soils* 51:113–122
- Zhang YS, Lin XY, Werner W (2003) The effect of soil flooding on the transformation of Fe oxides and the adsorption/desorption behavior of phosphate. *J Plant Nutr Soil Sc* 166:68–75
- Zhang ZJ, Zhang JY, He R, Wang ZD, Zhu YM (2007) Phosphorus interception in floodwater of paddy field during the rice-growing season in TaiHu Lake Basin. *Environ Pollut* 145:425–433
- Zhang M, Song G, Gelardi DL, Huang LB, Khan E, Masek O, Parikh SJ, Ok YS (2020) Evaluating biochar and its modifications for the removal of ammonium, nitrate, and phosphate in water. *Water Res* 186:116303